Stability vs flexibility: reshaping monolayer and bilayer archaeal membranes in silico

Miguel Amaral,[1,†] Felix Frey,[1,†] Xiuyun Jiang,[2] Buzz Baum,[3] and Anđela Šarić[1,*]

[1] *Institute of Science and Technology Austria, Klosterneuburg, Austria*
[2] *Department of Physics and Astronomy, University College London, London, UK*
[3] *MRC Laboratory of Molecular Biology, Cambridge, UK*

(Dated: October 18, 2024)

Across the tree of life, distinct designs of cellular membranes have evolved that are both stable and flexible. In bacteria and eukaryotes this trade-off is accomplished by single-headed lipids that self-assemble into flexible bilayer membranes. By contrast, archaea in many cases possess both bilayer and double-headed, monolayer spanning bolalipids. This composition is believed to enable extremophile archaea to survive harsh environments. Here, through the creation of a minimal computational model for bolalipid membranes, we discover trade-offs when forming membranes using lipids of a single type. Similar to living archaea, we can tune the stiffness of bolalipid molecules. We find that membranes made out of flexible bolalipid molecules resemble bilayer membranes as they can adopt U-shaped conformations to enable higher curvatures. Conversely, stiffer bolalipid molecules, like those found in archaea at higher temperatures, preferentially take on a straight conformation to self-assemble into liquid membranes that are stable, stiff, prone to pore formation, and which tear during membrane reshaping. Strikingly, however, our analysis reveals that it is possible to achieve the best of both worlds – membranes that are fluid, stable at high temperatures and flexible enough to be reshaped without leaking – through the inclusion of a small fraction of bilayer lipids into a bolalipid membrane. Taken together, our study compares the different membrane designs across the tree of life and indicates how combining lipids can be used to resolve trade-offs when generating membranes for (bio)technological applications.

Significance statement: All cells are bounded by a lipid membrane that needs to be both stable to function as a barrier and flexible to deform without leaking. Strikingly, two very different membrane designs have evolved to solve this problem. While bilayer membranes, assembled from single-headed lipids and typical of eukaryotes and bacteria, are relatively well studied, archaea have distinct membranes that often include both single and double-headed lipids. Here, through the development of a minimal computational model for archaeal membranes we discover conditions needed to create membranes that are stable and fluid at extreme temperatures, while being deformable at the same time. Taken together, our analysis reveals membrane design principles implemented in extremophiles that can be valuable for (bio)technological applications.

A bounding membrane separates the interior of every biological cell from its extracellular environment and gives the cell its shape. To perform its function, this bounding membrane must be sturdy and impermeable to the leakage of small charged molecules like ions to allow the generation of an electrochemical gradient [1], but also flexible enough to be remodelled during essential cellular processes like cell division and vesicle formation [2]. These requirements are partially conflicting and difficult to combine. Interestingly, two different generic membrane designs have evolved across the tree of life to solve this problem [3]. Bacterial and eukaryotic membranes possess fatty acid lipids that have a hydrophilic head group linked to hydrophobic tails via ester-linkages, which self-assemble into bilayer membranes [4]. By contrast, archaeal membranes lipids are constructed from branched isoprenoid lipids. These can include cyclopentane rings and which are attached via an ether linkage to one (e.g., archaeol, Fig. 1A left) or two hydrophilic heads, leading them to be called bipolar lipids or simply bolalipids (e.g., caldarchaeol, Fig. 1A right) [4]. As an ensemble,

† These authors contributed equally to this work
* Corresponding author: andela.saric@ist.ac.at

bilayer and bolalipids can self-assemble into fluid lipid membranes of different architectures - as bilayer lipid membranes, bolalipid membranes or mixture membranes (Fig. 1B right).

As a result of this distinct lipid composition and geometric organisations, archaeal membranes tend to have markedly different properties from eukaryotic and bacterial membranes. This feature of their membrane biochemistry is thought to be responsible, in part, for the ability of some archaea to survive under conditions like those found in volcanic springs at temperatures $> 75°$C, despite them lacking a cell wall. This hypothesis is supported by the observation that archaea alter their membrane composition depending on the environmental conditions to maintain a fluid but stable membrane [6]. Particularly, it has been found that at higher temperatures, the fraction of bolalipids in archaeal membranes increases [7], and bolalipids contain an increasing number of cyclopentane rings within their lipid tails, which can make the molecules more rigid and prone to aggregation [8]. For instance, the cell membrane of one of the standard archaeal model systems, Sulfolobus acidocaldarius, which lives at 80°C and pH 2, can contain over 90 % of bolalipids [8]. Besides temperature adaption, archaeal lipids also exhibit dense packing, high viscosity, and low porosity to small molecules like protons [9], enabling the Sulfolobus membrane to sustain pH gradients of 4 [10]. Intriguingly, some of the membrane-reshaping proteins which originated in archaea, such as ESCRTs [11] can also function with the membranes of eukaryotes, which are believed to have evolved as a merger between bacteria and archaea [12] and which have membranes made of bacterial lipids.

All this makes the study of reshaping archaeal membranes extremely interesting. Unfortunately, it is fairly challenging to investigate archaeal cells experimentally due to their unusual chemistry and extreme living conditions [13]. Therefore, most of what we know about archaeal tetraether lipid membranes thus far has been collected from studying *in vitro* reconstituted membranes. For instance, the conformation of individual lipids in bolalipid membranes was studied at the water-air interface [14] or using NMR experiments on lipid vesicles [15]. This suggested the existence of U-shaped lipid conformations in archaeal type membranes (Fig. 1B). X-ray studies further localized the head-groups to only one side of the layer, further supporting the existence of lipids within the membrane with a U-shaped conformation [16]. Membrane properties like bending stiffness [17] or lipid phase [18] have also been measured in vesicles prepared from archaeal tetraether lipids to demonstrate that archaeal lipid derived membranes are unique in being stable up to temperatures of 80°C [18]. Moreover, experiments with lipid vesicles made from synthetic bilayer lipids that include cyclopentane rings, which naturally appear in lipids of extremophilic archaea, showed that increasing the number of these rings increases membrane rigidity [19].

From the view point of membrane physics, the remodeling of bilayer membranes has been studied for decades using continuum models and computer simulations [20–22]. By contrast, apart from the aforementioned experimental studies and a few studies either using fine-grained MD simulations or theory [23–25], little research has been devoted to investigating the properties of archaeal bolalipid membranes despite the obvious importance of this question from evolutionary, biophysics, and biotechnological perspectives. Particularly, membrane reshaping at the mesoscale has been largely neglected although different membrane physics are expected to manifest.

To address this question, here we have designed a minimal model of archaeal membranes that can be used to explore the impact of both bolalipids and bilayer lipids on membrane biophysics and membrane reshaping. Our coarse-grained molecular dynamics simulations show that the geometry of bolalipids is, through the effects of entropy alone, sufficient to shift the fluid phase of archaeal-type membranes so that they are stable at high temperatures. In addition, we show that membranes assembled from bolalipids can have a much higher bending rigidity than bilayer-derived membranes, and are more likely to resist membrane shape changes as in fission. During membrane deformation, stress in these bolalipid membranes is relieved via a small fraction of bolalipids taking up a U-shaped conformation, which renders them a me-

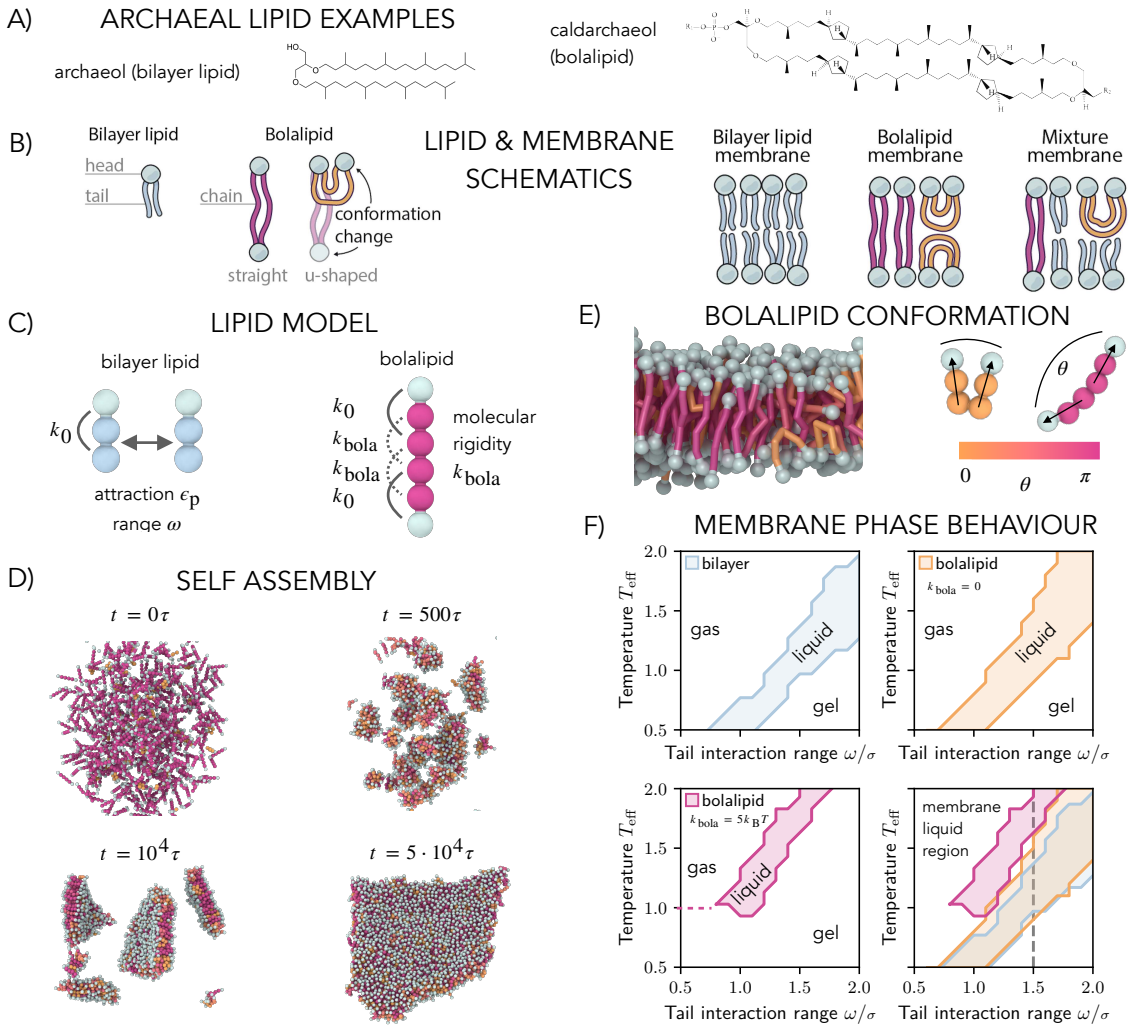

Figure 1. **Computational model and phase space of bilayer and bolalipid membranes.** (A) Structure of the diether bilayer lipid archeol (left) and the tetraether bolalipid caldarchaeol including four cyclopentane rings (right), both present in the membrane of *Subfolobus acidocaldarius*, a common archaeal model system that lives at high temperatures and low pH [5]. (B) Schematics for a bilayer lipid, a bolalipid and its two in-membrane conformations, membranes made of bilayer molecules only, bolalipid molecules only, and a mixture of the two (left to right). (C) Bilayer lipid (left) is described with one head bead and two tail beads straightened by an angular potential of strength k_0. Tail beads of different lipids attract with the strength ϵ_p and the range ω. Bolalipids (right) consist of two bilayer lipids connected by a bond and straightened by an angular potential of strength k_{bola}. (D) Snapshots of bolalipids self-assembling into a flat membrane ($k_{bola} = 0.3\, k_B T$). (E) Cross-section of self-assembled membrane (right), with bolalipids colored according to their conformation: straight lipid in crimson and u-turn lipid in orange. (F) Membrane phase behavior: liquid, gel and gas regions as a function of the effective temperature T_{eff} and tail interaction range ω for bilayer (top left) and membranes made of flexible $k_{bola} = 0$ (top right) and stiff $k_{bola} = 5\, k_B T$ (bottom left) bolalipid molecules. Overlays of all liquid regions (bottom right) show that stiffer lipids exhibit fluid membrane region at higher temperatures. The dashed line marks $\omega = 1.5\sigma$, the value we used in the rest of the work.

chanically switchable material, or by the formation of large pores. Remarkably, however, when combined, a mixture of bilayer and bolalipids generates membranes that are stable at high temperature, which becomes softer as the fraction of bilayer lipids increases. Taken together, our results demonstrate how doping a bolalipid membrane with a small fraction of bilayer lipids can relieve the trade-off, enabling membranes to be both stable under extreme conditions and to be remodelled without leaking.

RESULTS

Computational Model. To study bolalipid membranes and compare them to bilayers, we extended the Cooke and Deserno model for bilayer membranes [26]. In the original model for the bilayer a single bilayer lipid is represented by a chain of three nearly equally sized beads of diameter of $\sim 1\sigma$, where σ is our distance unit and roughly maps to 1 nm (Fig. 1C left); one bead stands for the head group (cyan) while the others represent the hydrophobic tail (blue). Each adjacent pair of beads in a lipid is linked by a finite extensible nonlinear elastic (FENE) bond. The angle formed by the chain of three beads is kept near 180° via an angular potential with strength k_0. While lipid heads interact exclusively through volume exclusion, the beads of lipid tails interact via a soft attractive potential of the strength ϵ_p and range ω (Fig. 1C left), effectively modelling hydrophobic interaction in an implicit solvent. This interaction strength governs the membrane phase behavior and can be interpreted as the effective temperature $T_\mathrm{eff} = k_\mathrm{B}T/\epsilon_\mathrm{p}$.

To model a bolalipid molecule, we joined two bilayer lipids so that a lipid molecule is formed with a head bead (cyan) that is linked to four tail beads (crimson) which are again linked to another head bead (Fig. 1C right). In this way, both bilayer lipids and bolalipids share the same molecular structure and the same interactions between lipid beads. Bolalipids in archaeal membranes can differ in the number of cyclopentane rings or the branching of the tail and thus in the molecular stiffness [6, 27]. To represent this effect, we added two angular potentials between the second and the fourth and the third and the fifth tail bead with variable strength k_bola. By varying k_bola, we can control the molecular stiffness of the bolalipid molecules and thus model different types of bolalipids. The model is simulated within molecular dynamics implemented in the LAMMPS open source package [28], and simulations are visualized with OVITO [29]. To include the implicit effect of the surrounding water and to simulate membranes at vanishing tension, we used a Langevin thermostat combined with a barostat that kept the membrane in the x-y plane at zero pressure. Details on the computational model are given in the Supplemental Information (SI) section 1.

Self-assembly and phase behavior. We first tested the ability of both the bilayer and bolalipid molecules to self-assemble into membranes. To do so, we placed dispersed lipids in a periodic 3D box. For both bilayer and bolalipids we found that membranes self-assembled over a wide range of lipid interaction parameters (Fig. 1D, SI section 2, and Movie S1). We then explored the influence of flexibility in the bolalipid molecule. At small values of the molecular rigidity k_bola, single lipids are flexible and can thus adopt a range of possible conformations. The different conformations can be classified by the angle θ between the two lipid heads (Fig. 1E). Two lipid conformations dominated the conformation distribution in the context of a membrane: the U-shaped conformation with both head beads on the same membrane leaflet ($\theta \approx 0$) and the straight conformation with one head bead in opposing membrane leaflets ($\theta \approx \pi$) (Movie S2.b, Fig. S1, and SI section 3; for comparison, bilayer membranes in Movie S2.a and rigid bolalipid membranes in Movie S2.c). In the self-assembled bolalipid membrane, we marked bolalipids as being in the U-shape conformation if $\theta < \pi/2$ and in the straight conformation otherwise.

To study the phase behavior of bilayer and bolalipid membranes, we analyzed the diffusion of single lipids in self-assembled membranes as a function of the lipid interaction parameters ϵ_p and ω (SI sections 4 and 5). The diffusion con-

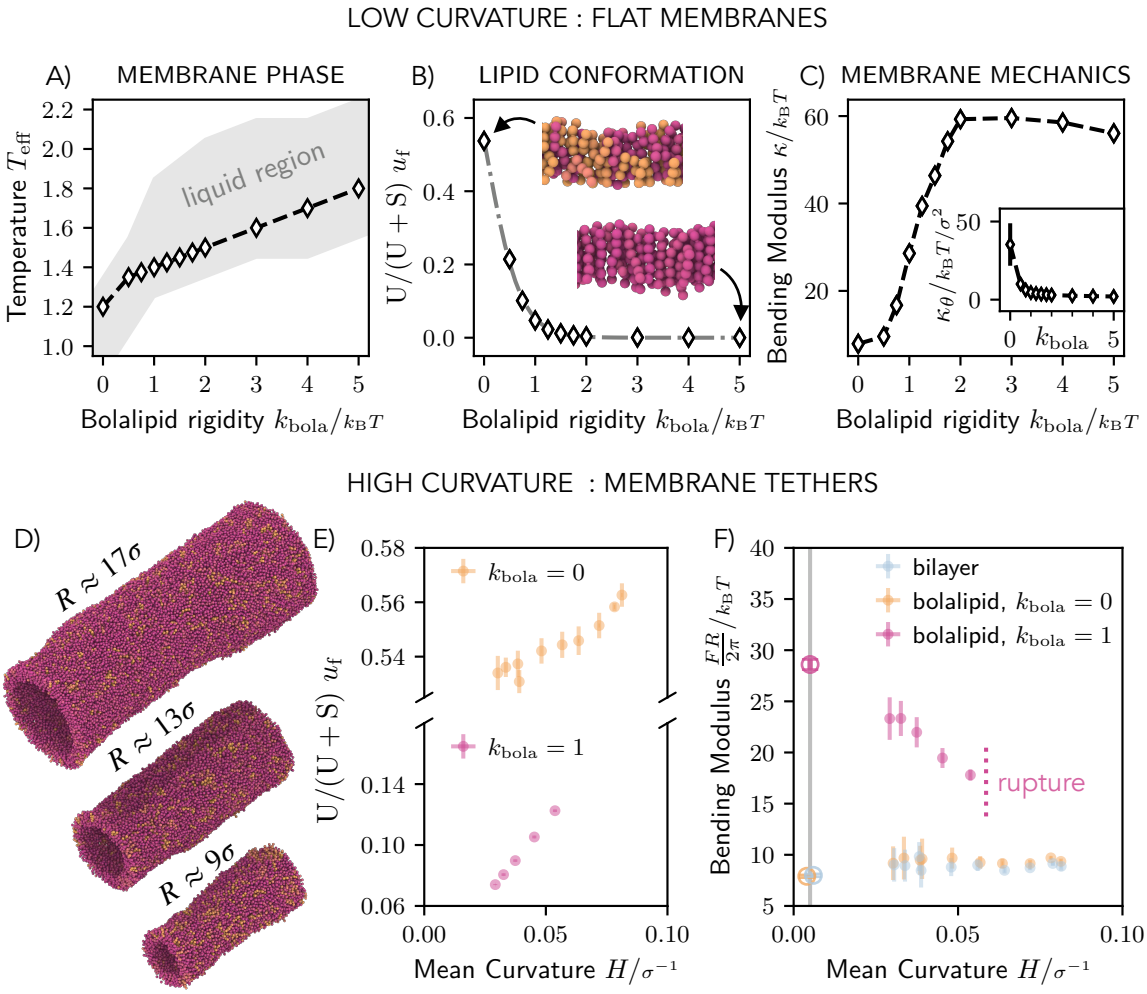

Figure 2. **Mechanics of pure bolalipid membranes.** (A) Liquid region as a function of temperature and bolalipid rigidity for pure bolalipid membranes (gray). The dashed line shows the bolalipid membranes of approximately same fluidities. (B) Fraction of bolalipids in the U-shape conformation ($\theta = 0$), fitted to $u_{\mathrm{f}}(k_{\mathrm{bola}}) = 1/(1 + \exp(\beta(-0.16 + 3k_{\mathrm{bola}})))$ (gray dashed line) according to a two-state model. Insets: simulation snapshots with bolalipids colored according to their conformations. (C) Bending modulus as a function of bolalipid molecule rigidity k_{bola}. Inset: Tilt modulus as a function of bolalipid rigidity k_{bola}. (D) Snapshots of bolalipid membranes at the range of explored curvatures for $k_{\mathrm{bola}} = 1k_{\mathrm{B}}T$. (E) Fraction of bolalipid molecules in the U-shaped conformation as a function of the mean membrane curvature $H = 1/(2R)$ for membranes made of flexible ($k_{\mathrm{bola}} = 0$) and semi-flexible ($k_{\mathrm{bola}} = 1k_{\mathrm{B}}T$) bolalipid molecules. (F) Bending modulus as a function of curvature. For the flat membrane ($H \sim 0$), the corresponding bending rigidity from (C) is marked by the vertical line and empty circles.

stant D exhibited a discontinuity as a function of the temperature, which marks the transition as the membrane moves from the gel phase to the liquid phase. The discontinuity occurred at different values of interaction strength ϵ_{p} and interaction range ω for bilayer and bolalipid lipids, and it also depended on the values of the molecular stiffness k_{bola} (Fig. S4). In these simulations, the disintegration of the membrane defined an upper limit to the liquid phase and the transition to the gas phase. Based on this classification, we plotted the phase diagram for bilayer membranes (Fig. 1F top left), fully flexible bolalipid membranes ($k_{\mathrm{bola}} = 0$, Fig. 1F top right), and rigid bolalipid membranes ($k_{\mathrm{bola}} = 5\,k_{\mathrm{B}}T$, Fig. 1F bottom left) as a function of the range of the hydrophobic interaction ω and the temperature T_{eff}. Membranes made of bilayers (blue) and flexible bolalipid molecules ($k_{\mathrm{bola}} = 0$, orange) behaved similarly under these conditions (Fig. 1F bottom right). Strikingly, just as observed in extremophile archaea, as the molecular stiffness of bolalipids increased ($k_{\mathrm{bola}} = 5\,k_{\mathrm{B}}T$, magenta), the liquid region was shifted toward higher temperatures and larger values of the interaction range. This is due to the fact that bolalipid molecules are able to engage in more extensive interactions with partners when in the extended conformation, which helps to stabilize the membrane at higher temperatures.

Bolalipid conformations and mechanical properties. To explore mechanical properties of bolalipid membranes, we chose $\omega = 1.5\,\sigma$ for the remainder of the work (dashed line in Fig. 1F bottom right). Fig. 2A shows the phase diagram for bolalipid membranes replotted as a function of temperature and bolalipid rigidity for the chosen interaction range. To be able to compare membranes made of bolalipids of different molecular rigidities, we needed to adjust temperature for each to reach similar fluidities, shown by dashed lines in Fig. 2A. We then characterised the conformations of individual bolalipids in flat membranes, measured by the fraction of bolalipids in U-shape conformation u_{f}. We find that for flexible bolalipids ($k_{\mathrm{bola}} = 0$), more than 50% of all lipids are in the U-shape conformation (Fig. 2B). This fraction decreases with increasing rigidity of bolalipid molecules and and vanishes around $k_{\mathrm{bola}} \geq 2\,k_{\mathrm{B}}T$, for which almost all bolalipids take up linear conformations.

This behavior can be easily captured by considering bolalipids as a two state system, with straight and U-shape conformation, as argued before (Fig. S1). We assumed that the energy of the straight conformation vanishes $E_{\mathrm{s}} = 0$ and the energy of the U-shape conformation reads $E_{\mathrm{u}} = c_0 + c_1 k_{\mathrm{bola}}$, where, for simplicity, we assumed that the energy linearly depends on k_{bola} which is the only relevant energy scale in the system and the two constants c_0 and c_1, which determine the conformation energy of U-shaped bolalipids. The fraction of bolalipids in U-shape conformation then follows $u_{\mathrm{f}}(k_{\mathrm{bola}}) = 1/(1 + \exp(\beta(c_0 + c_1 k_{\mathrm{bola}})))$, with $\beta = 1/(k_{\mathrm{B}}T)$, as shown by the fit in Fig. 2B (dashed gray line, $R^2 = 0.99$, see SI section 6). For the fit it appears that $c_0 < 0$, which implies that bolalipids in U-shape conformation are slightly favored over straight bolalipids at $k_{\mathrm{bola}} = 0$ likely because of entropic reasons.

Bolalipid conformations and membrane rigidity. It was previously hypothesized that an increasing fraction of bolalipids in straight configuration would increase the membrane rigidity [17]. To determine the membrane rigidity using our model, we assessed the height fluctuation spectrum (h^2) of flat membranes in a periodic box. [26, 30]. Interestingly, we found that the original theory of Helfrich [31] failed to describe the resulting height fluctuation spectrum. However,the extended theory by Hamm and Kozlov [32], which also includes the energetic cost of lipid tilt, successfully captured bolalipid fluctuations. In this case, the resulting height spectrum of the membrane at vanishing membrane tension is given by [30]

$$\begin{aligned}\langle |h_n|^2 \rangle &= \frac{k_{\mathrm{B}}T}{L^2}\left(\frac{1}{\kappa q^4} + \frac{1}{\kappa_\theta q^2}\right) \\ &= \frac{k_{\mathrm{B}}T}{L^2}\frac{1}{\kappa}\left(\frac{1}{q^4} + \frac{l_\theta^2}{q^2}\right), \qquad (1)\end{aligned}$$

where $q = 2\pi n/L$ is the wave number, L is the box size, κ is the bending rigidity of the membrane, κ_θ is the tilt modulus and $l_\theta = \sqrt{\kappa/\kappa_\theta}$

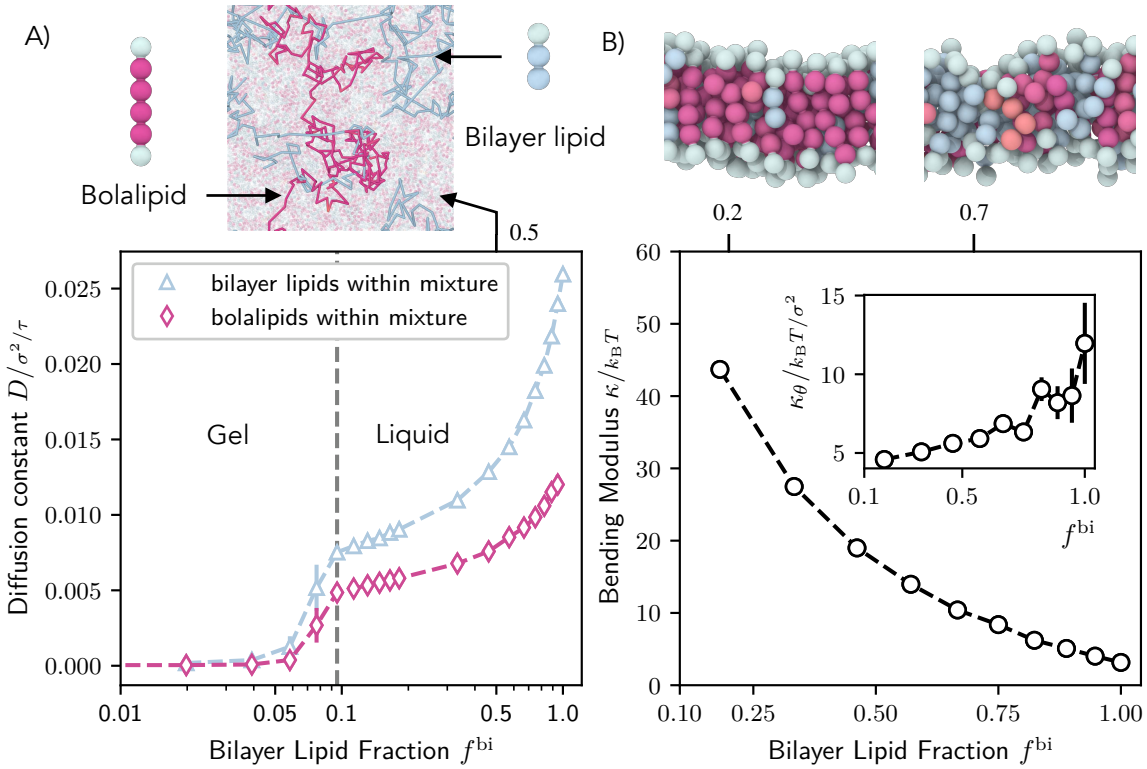

Figure 3. **Fluidity and rigidity of mixed bilayer/bolalipid membranes.** (A) Single lipid diffusion constant for each species as a function of bilayer fraction f^{bi} (measured by the head beads fraction; $k_{\mathrm{bola}} = 2k_{\mathrm{B}}T$, $T_{\mathrm{eff}} = 1.3$). For $f^{\mathrm{bi}} \geq 0.1$, the resulting mixture becomes liquid. Top: Diffusion trajectories of a bolalipid (blue) and a bilayer lipid (red) in a mixture membrane at $f^{\mathrm{bi}} = 0.5$. (B) Bending rigidity κ and (Inset) tilt modulus κ_θ as a function of the fraction of bilayer molecules f^{bi}. Top: Snapshots show bilayer lipids (blue) in mixed membranes at two different values of f^{bi}.

is a characteristic length scale related to tilt. Considering Eq. (1), the tilt term is expected to matter if the analyzed inverse wave numbers become similar to l_θ. The wave numbers that we analyzed correspond to wavelengths that are at least twice the thickness of the membrane ($q < 2\pi/(12\sigma) \approx 0.5\,\sigma^{-1}$). Thus, the tilt term is expected to contribute if $l_\theta > 2\,\sigma$. For typical bilayer membranes, one finds $\kappa_\theta = 12\,k_{\mathrm{B}}T\,\mathrm{nm}^{-2}$ [30] and $\kappa = 20\,k_{\mathrm{B}}T$ [33], so $l_\theta \sim 1\,\mathrm{nm} \approx 1\,\sigma$ and therefore the tilt term can be neglected as practiced before [26]. However, when the membrane rigidity increases as we expect for bolalipid membranes, l_θ increases and the tilt term in Eq. (1) becomes relevant.

By fitting the height spectrum for bolalipid membranes (and bilayer membranes for comparison) (Fig. S6), we measured the bending rigidity (Fig. 2C) and tilt modulus (Fig. 2C inset) as a function of k_{bola} (see SI section 7 and Movie S3). With increasing bolalipid molecular rigidity k_{bola}, the bending rigidity κ rose from $8\,k_{\mathrm{B}}T$ and plateaued at $60\,k_{\mathrm{B}}T$, showing bolalipid membranes can be very rigid while liquid. Strikingly, the increase in membrane rigidity coincided with U-shaped bolalipids vanishing from the membrane (Fig. 2B), which confirmed the hypothesis that straight

bolalipids render lipid membranes rigid. At the same time, the tilt modulus κ_θ decreased with bolalipid rigidity, from $30 \pm 10\, k_\mathrm{B}\, T/\sigma^2$ to $2\, k_\mathrm{B}\, T/\sigma^2$, lowering less than $1\, k_\mathrm{B}\, T$ for $k_\mathrm{bola} \geq 2\, k_\mathrm{B}\, T$. Since membrane bending and lipid tilting are two modes of membrane deformations that compete, we conclude that bilayer and flexible bolalipids molecules form flexible membranes that prefer to bend rather than to tilt, while bolalipids in straight configuration form rigid membranes that prefer to tilt rather than to bend. Taken together, bolalipid membranes made of flexible lipid molecules are as flexible as lipid bilayers, adopting U-shaped conformations, where those made of bolalipids in straight configurations are rigid.

Interplay between membrane curvature and rigidity. Following geometric intuition, we expect the fraction of molecules in the U-shape to change as the membrane curvature changes, to enable area difference between the two membrane leaflets needed to adopt to the curvature. This would imply that the bending rigidity, importantly, through the fraction of U-shaped bolalipids, is curvature dependent. To investigate the impact, we measured the bending rigidity of bolalipid membranes in cylindrical shapes as a function of their radii [34] (see Fig. 2D, Movie S4, and SI section 8). We first noticed that while membrane tubes made of bilayer and flexible bolalipids were stable up to small cylinder radii R, almost as small as the membrane thickness itself, we found that membrane made from stiffer bolalipids ($k_\mathrm{bola} = 1 k_\mathrm{B}\, T$) ruptured well before. Strikingly, while for stiffer bolalipids ($k_\mathrm{bola} = 1 k_\mathrm{B}\, T$) the U-shaped bolalipid fraction increased strongly over a short range of the mean membrane curvature ($H = 1/(2R)$), we only found a small change in the U-shaped bolalipid fraction of flexible bolalipid membranes ($k_\mathrm{bola} = 0$) (Fig. 2E). Consequently, since the fraction of U-shaped bolalipid molecules controls the bending rigidity of bolalipid membranes (Figs. 2B and 2C), we found that there is a strong dependency of the bending rigidity κ on the membrane mean curvature of stiffer bolalipids ($k_\mathrm{bola} = 1 k_\mathrm{B}\, T$) (Fig. 2F). In contrast, we did not find that κ was curvature-dependent for bilayer or flexible bolalipid membranes ($k_\mathrm{bola} = 0$). Taken together, the rigidity of bolalipid membranes is not only controlled by the molecular stiffness of their lipid constituents but also by the emerging geometry of the ensemble of lipids. Since membrane geometry and thus membrane rigidity will change upon membrane deformations this gives rise to plastic material properties.

Gaussian rigidity of bolalipid membranes. Another important material parameter is the Gaussian bending modulus $\bar{\kappa}$, which characterizes the reshaping behavior of fluid lipid membranes under topological changes [33]. $\bar{\kappa}$ is notoriously difficult to measure since it only becomes detectable when the membrane changes its topological state. Continuum membrane theory, combining stability arguments and elasticity, predicts $-\bar{\kappa}/\kappa \in [-0.5, -1]$ [33], where the former value is expected for incompressible membranes. Indeed, most of the numbers we know for the ratio of the two bending rigidities, many of which were deduced from simulations, lie within this range [35]. Using the same method as developed by Hu et al. [35], we determined $\bar{\kappa}$ by measuring the closing efficiency of membrane patches into a sphere (see SI section 9). We obtained $\bar{\kappa} = -4.61 \pm 1.91\, k_\mathrm{B}\, T$ and thus a ratio of $-\bar{\kappa}/\kappa = 1.07 \pm 0.50$ for bilayer membranes. In contrast, we got significantly larger values (less negative) with $\bar{\kappa} = -2.81 \pm 2.41\, k_\mathrm{B}\, T$ and $-\bar{\kappa}/\kappa = 0.55 \pm 0.49$ for flexible bolalipid membranes ($k_\mathrm{bola} = 0$). The result shows that in addition to the differences in bending rigidities, the ratio of the two bending moduli differs strongly in bilayer and bolalipid membranes.

Archaeal membranes made of mixtures of bolalipids and bilayer-forming lipids. Archaeal membranes contain varying amounts of bilayer lipids [8, 36]. The exact bolalipid/bilayer fraction depends on the growth temperature, with higher levels of bolalipids with increasing temperature [7], and higher fraction of cyclopentane rings in the tails [27]. In order to investigate the effect of different lipid contents on membrane mechanical properties, we wanted to model the archaeal membrane by

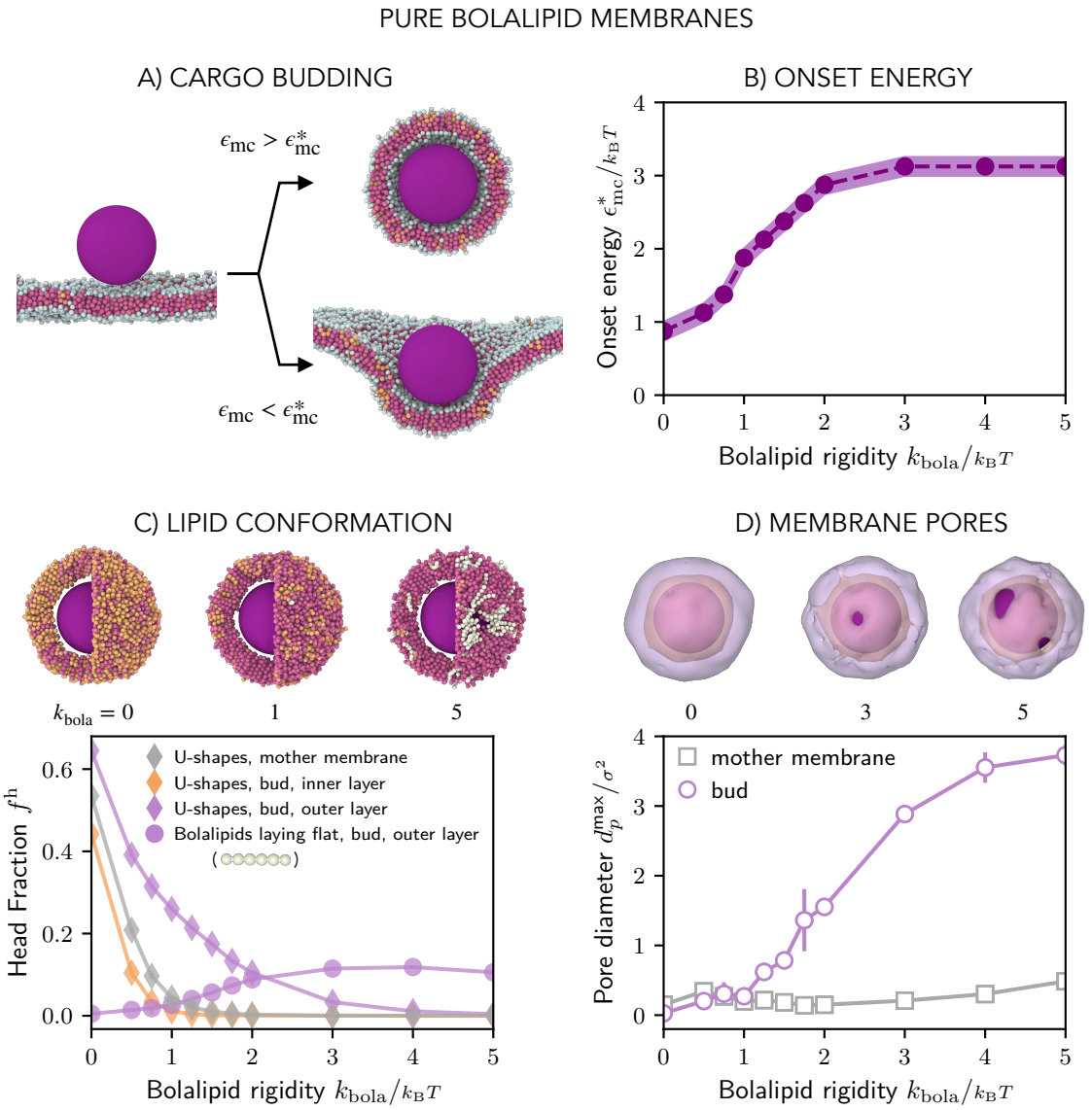

Figure 4. **Reshaping of pure bolalipid membranes.** (A) Simulation snapshots of the membrane wrapping a cargo bead adsorbing onto it. Above the onset adsorption energy ϵ^*_{mc}, the cargo is fully wrapped by the membrane and buds off the mother membrane. (B) Onset energy ϵ^*_{mc} as function of the bolalipid molecule rigidity k_{bola} (for the parameters defined by the line in Fig. 2A). (C) Bottom: Fraction of bolalipids in the U-shape conformation u_f in the outer and inner layers of the membrane bud, and in the flat mother membrane, as function of the bolalipid molecule rigidity k_{bola}. Top: Snapshots and cross-sections of the membrane around the cargo bud. At high bolalipid rigidity the pores form around the cargo, and are lined with bolalipid molecules lying flat around the pore in a straight conformation, with both heads in the outer layer (colored in white). The rest of bolalipids colored according to their head-to-head angle as before. (D) Bottom: Average diameter of transient pores in the membrane bud and the mother membrane as function of the bolalipid molecule rigidity k_{bola}. Pores are defined as membrane openings through which a sphere of diameter 1σ can cross. Top: Snapshots of the membrane surface with outer and inner leaflet surface colored in purple and orange, respectively, intersecting at the rim of the pore (gray).

mixing bilayer lipids into bolalipid membranes. Since in our model, the liquid regions of rigid bolalipid membranes and bilayer membranes do not overlap (Fig. 1F bottom right), we picked the temperature $T_{\mathrm{eff}} = 1.3$ to minimize fluidity mismatch and we set the molecular rigidity $k_{\mathrm{bola}} = 2\,k_{\mathrm{B}}T$ to limit U-shaped bolalipids (Fig. 2B). We then measured the diffusion constant D as a function of the fraction of bilayer lipids f^{bi} (see SI section 5). Interestingly, we found that mixing only 10% bilayer lipids into the bolalipid membrane in gel state is enough to fluidize the membrane (Fig. 3A). We then measured the bending rigidity and the tilt modulus of flat mixture membranes by analyzing the fluctuation spectrum. While the bending rigidity κ decreased (Fig. 3B), the tilt modulus increased non-linearly with the bilayer lipid fraction f^{bi} (Fig. 3B inset). Taken together, the bolalipid membrane can be substantially softened either through bolalipids acquiring U-shaped conformation or through addition of bilayer-forming lipids.

Curving bolalipid membranes. To investigate the response of bolalipid membranes to large membrane curvature and topology changes like those induced upon vesicle budding, which regularly occurs in archaea, we simulated membrane wrapping of an adhesive cargo bead (Fig. 4A, Movies S5.a to S5.c, and SI section 10). Importantly, this provided us with a method to study how lipid organization is affected by externally imposed membrane curvature and mechanics. We first simulated membrane wrapping at different adsorption energies ϵ_{mc} between lipid head beads and the cargo until we observed that the membrane wrapped the cargo completely (including membrane fission). Then the minimum adsorption energy, for which a membrane bud completely enveloped the cargo bead, is the onset adsorption energy ϵ^*_{mc} (Fig. 4A), which we measure as a function of the bolalipid stiffness k_{bola} (Fig. 4B). For small molecular stiffness k_{bola}, ϵ^*_{mc} first increases linearly with k_{bola} before it saturates around $k_{\mathrm{bola}} = 3\,k_{\mathrm{B}}T$. We expect that the onset energy is proportional to the membrane bending rigidity $\epsilon^*_{\mathrm{mc}} \propto \kappa$, because the bending energy to wrap a spherical particle is size-invariant [33, 37]. When we increased the bending rigidity, through increasing stiffness of bolalipid molecule k_{bola}, ϵ^*_{mc} increased by a factor of 3 (Fig. 4B), suggesting that also κ increased by a factor of 3. However, from directly measuring the membrane rigidity from the fluctuation spectrum (Fig. 2C), we saw that κ increased by a factor of 10. To reconcile these seemingly conflicting observations we reason that the bending rigidity κ, similar to Fig. 2F, is not constant but softens upon increasing membrane curvature, due to dynamic change in the ratio between bolalipids in straight and U-shaped conformation. Hence, bolalipid membranes show stroking plastic behavior as they soften during reshaping.

Through analysing the bolalipid conformations, we found that the membrane was able to curve by increasing the fraction of U-shaped bolalipids in the outer layer of the deformation (Fig. 4C and SI section 12). To a lesser degree, we also observed this effect on the inner membrane neck (Fig. S12). Remarkably, though, even when lipids are so stiff that there are no more U-shaped bolalipids in the flat mother membrane ($k_{\mathrm{bola}} = 2\,k_{\mathrm{B}}T$), the outer layer of the a curved membrane retained a non-negligible fraction of $\approx 10\%$ U-shaped bolalipids, which in turn decreases κ and softens the membrane. However, the softening effect on the membrane, indicated through a constant onset energy for $k_{\mathrm{bola}} \geq 3\,k_{\mathrm{B}}T$ (Fig. 4B), persists even for those very stiff bolalipids. Since for stiff membranes, practically all U-shaped bolalipids are gone (Fig. 4C), this suggested that an additional membrane-curving mechanism must be involved.

Looking more closely, at high molecular rigidity ($k_{\mathrm{bola}} \geq 2k_{\mathrm{B}}T$) we observed the formation of multiple pores on the membrane bud, which we quantified by measuring the time-averaged maximum pore diameter (Fig. 4D, see SI section 12 and Movie S6). While large pores were not observed in the flat membrane, the diameter of membrane pores around the cargo was found to grow with the increase in bolalipid stiffness. We reasoned that pores form when the energetic cost required to change the bolalipid conformation to release bending stress is larger than the energetic cost of opening a lipid edge

surrounding the pore. Hence, for relatively flexible bolalipids, U-shaped bolalipids provide the necessary area difference between the outer and inner layer of the membrane bud and thereby soften the membrane. For stiff bolalipid molecules, however, membrane pores start to form to enable membrane curvature as U-shaped bolalipids become prohibited. Both mechanisms help to explain the discrepancy between ϵ^*_{mc} and the bending modulus κ obtained by studying membrane fluctuations (Fig. 2C).

Curving archaeal membranes. Having shown that bolalipid membranes can effectively soften also by including some amount of bilayer-forming lipid molecules, we next measured the onset energy ϵ^*_{mc} for cargo budding in the membranes formed by mixtures of bolalipids and bilayer-forming lipids, as a function of bilayer lipid fraction f^{bi} (Fig. 5A and Movie S5.d). We found that the onset energy sharply decreases with increasing amount of bilayer forming lipids, and plateaus for 50% bilayer fraction, where it acquires similar values as in the case of fully-flexible bolalipids (Fig. 4B). For small bilayer lipid fractions, U-shaped bolalipids localize almost exclusively on the outer layer of the bud (Fig. 5B). As the bilayer fraction increases, there is a steady reduction in the percentage of U-shaped bolalipids in the outer layer in favor of bilayer lipids that take their role in supporting membrane curvature, with U-shaped bolalipids completely vanishing at high fractions of bilayer-forming lipids. A fraction of bilayer lipid head beads initially shows an asymmetry between the preferred outer layer and the penalized inner layer around the cargo (Fig. 5C), but eventually approaches f^{bi} in both layers. Taken together, as the bilayer lipid fraction increases, the role of U-shaped bolalipids in making up the asymmetry between the outer and inner layer, is taken over by bilayer lipids. Curiously, the addition of bilayer lipids promotes the formation of U-shaped lipids, both in the flat membrane and even in the inner layer around the bud. This is likely to be explained by the fact that when more bilayer lipids are incorporated, the membrane is less densely packed (Fig. S10B) and thus U-shaped bolalipids are promoted.

Importantly, we observed nearly no pores in the membrane bud in mixed membranes, even when we only had very little fraction of bilayer-forming lipids (Fig. 5D). Only as the bilayer fraction increased, we observed the formation of very small pores in the bud. For the flat mother membrane, however, membrane pores started to form with increasing values of f^{bi}. They acquired sizes similar to those obtained around the bud in pure bolalipid membranes (Fig. 4D). The pore formation in the flat mother membrane is likely promoted because the membrane becomes destabilized by the increasing proportion of bilayer lipids which are close to the gas phase. Taken together, bolalipids can bud porelessly when bilayer-forming lipids, which cause membrane softening, are included.

Discussion. All biological cells are enclosed in fluid lipid membranes. These must be both sturdy and flexible to contain the cellular interior and allow membrane reshaping during division and vesicle formation. Across nature, mono- and bilayer membranes, composed of bilayer and bolalipids have evolved that allow to fulfill these partially conflicting requirements. In this work, we have developed the first minimal model that allows us to transparently compare the distinct behavior of bilayer and bolalipid membranes. In our model, bolalipids are formed by joining together two bilayer lipids, with an adjustable molecular stiffness at the hinge point. Using our model we find striking differences between bilayer and bolalipid membranes in terms of stability, rigidity and plasticity. Our results highlight how bolalipid membrane behave effectively as two-component systems, exchanging bolalipids between different conformations and thereby allowing the material properties to be adapted to support membrane reshaping.

While flexible bolalipid membranes are liquid under the same conditions as bilayer membranes, we found that stiff bolalipids form membranes that operate in the liquid regime at higher temperatures. These results agree well with previous molecular dynamics simulations that suggested that bolalipid membranes are more ordered and have a reduced diffusivity

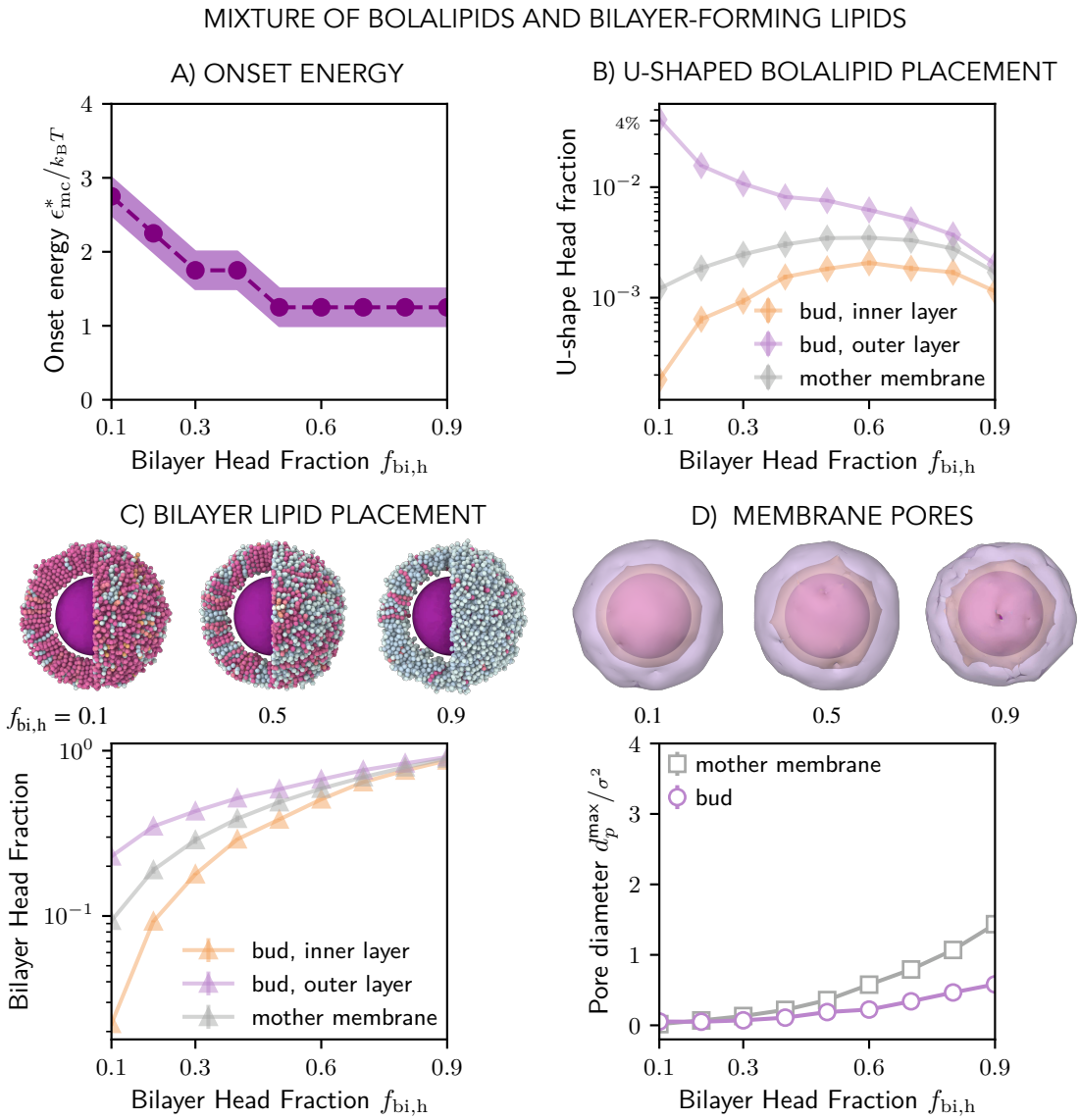

Figure 5. **Curving of the mixed membranes, made of bilayer and bolalipid molecules.** (A) Onset energy required to form the membrane bud, $\epsilon^*_{\rm mc}$, as function of bilayer fraction $f^{\rm bi}$ (for the parameters defined in Fig. 3.) (B and C) Fraction of U-shaped bolalipid molecules $u_{\rm f}$ (B) and bilayer molecules (C) in the outer and inner layers of the membrane bud and in the flat mother membrane as a function of the bilayer fraction $f^{\rm bi}$. Top panels show the respective snapshots of membrane surface around cargo, where bilayer lipids are shown in light blue as in Fig. 4. (D) Average diameter of transient pores in the membrane bud and the mother membrane as function of bilayer fraction $f^{\rm bi}$ and respective snapshots of membrane leaflet surfaces surrounding the bud (Top panel).

compared to bilayer membranes [23, 24]. In our simulations, this is due to the fact that completely flexible bolalipids molecules adopt both straight (transmembrane) as well as the U-shaped (loop) conformation with approximately the same frequency. In contrast, stiff bolalipids typically only take on the straight conformation when assembled in a membrane. These results agree with the previous coarse-grained molecular dynamics simulations using the MARTINI force field which showed that the fraction of straight to U-shaped bolalipids increased upon stiffening the linker between the lipid tails [23].

When we determined the bending rigidity of bolalipid membranes by measuring their response to thermal fluctuations, we found that membranes made from flexible bolalipids are only slightly more rigid than bilayer membranes. This result is consistent with previous atomistic simulations, which showed that the membrane rigidity was similar for membranes composed of bilayer lipids and flexible synthetic bolalipids [38]. Moreover, the result is consistent with a continuum theory which predicted that the rigidity of membranes formed of triblock copolymers is 20% larger than that of diblock copolymers [39]. However, bolalipids in extremophilic archaea are not predicted to be fully flexible as they are expected to pack tighter due to a large number of cyclopentane rings in the lipid tails [6, 27]. Indeed, we found that membranes made of stiff bolalipid molecules can exhibit stiffness that is more than an order of magnitude larger than that of bilayer lipids at the same membrane fluidity.

It is striking that membranes made from stiffer bolalipids showed a curvature-dependent bending modulus, which is a clear signature that bolalipid membranes exhibit plastic behavior during membrane reshaping. Another marked difference between bilayer and flexible bolalipid membranes is that the Gaussian bending rigidity is almost twice as large as that of bilayer lipids and the ratio of the bending modulus to Gaussian rigidity is around 1/2. It is not obvious how the Gaussian bending modulus would behave upon increasing bolalipid stiffness ($k_{\mathrm{bola}} > 0$), or how to measure it due to the coupling between curvature and rigidity in bolalipid membranes. In any case, our results indicate that membrane remodelling, such as membrane fission during membrane traffic, is much more difficult in bolalipid membranes [33]. It is tempting to speculate that this is one of the reasons why eukaryotes use bilayer membranes, enabling dynamic membrane remodelling and trafficking.

It is interesting to draw a parallel between monolayer membranes made of stiff bolalipid molecules and macroscopic membranes composed of rigid straight colloidal particles, which are geometrically similar, but living at different scales [40]. It has been found that colloidal membranes at these macroscopic scales follow the standard Helfrich theory for bilayer membranes [41], with rigidity that is three orders of magnitude higher than those of lipid bilayers [42]. In this case the tilt modulus was not pertinent, likely due to macroscopic system sizes. Similarly, we expect that the bending rigidity can be determined from membrane fluctuations independently of the tilt modulus for bolalipid membranes if they are prepared at similar relative sizes. Beyond quantitative differences, the comparison shows that monolayer membranes follow the same physics across many orders of magnitudes. However, when considering subcellular scales and the formation of high curvature, as in vesicle budding, the tilt modulus and thus the substructure of the membrane is expected to matter.

We found that membranes formed of a mixture of bilayer and bolalipids, similar to archaeal membranes, function as a composite liquid membrane that softens when adding bilayer lipids. However, while in our simulations the bending rigidity monotonically decreases with bilayer fraction, previous experiments of mixture membranes of bilayer and bolalipids with cyclopentane rings suggested that the bending rigidity non-monotonically depends on the fraction of the membrane made up of bilayer lipids [17]. It remains to be determined whether the result is due to the specific lipids used, the resulting mismatch in lengths between two stacked bilayer lipids and a straight bolalipid, the experimental conditions or to non-linear effects such as the formation of lipid domains that soften the membrane with increasing bolalipid content. The same experiments reported that membranes consisting solely of bolalipids are

more rigid than bilayer membranes and non-fluctuating, which is in agreement with our high bending modulus simulation results for near-pure bolalipid mixture membranes.

To investigate how bolalipid membranes respond to changing membrane curvature, we performed simulations in which small cargo particles budded from flat membranes. We found that by enforcing curvature on bolalipid membranes, the fraction of U-shaped bolalipids increased around the cargo bud, especially in the outer membrane layer and hence softened the membrane. As another mechanism to release curvature stress we observed the formation of membrane pores, which could be mended by adding small amounts of bilayer lipids, similar to the mixture membranes that are found in archaea [36]. Our results suggest that enforcing membrane bending can soften bolalipid membranes locally by increasing the number of U-shapes, rendering the membrane a mechanically switchable material where large curvature decreases stiffness.

Taken together, our results show how membranes which are mixtures of bilayer and bolalipids maintain cell integrity at high temperatures, while also undergoing leak free membrane bending. This suggest that archaeal membranes can balance opposing needs when adapting to extreme environmental conditions. Beyond understanding membrane properties and reshaping across the tree of life, these results pave the way for synthetic bolalipid membranes and bolalipid membrane containers with new and exciting material properties.

AUTHOR CONTRIBUTIONS

MA performed computer simulations and analysis and wrote the manuscript. FF performed patch closing simulations, contributed to computer simulations and analysis, and wrote the manuscript. XJ contributed to budding simulations and the manuscript. BB co-supervised the project and edited the manuscript. AŠ conceived the study, supervised the project and edited the manuscript.

DATA AVAILABILITY

The simulation input files and codes are freely available at [43].

ACKNOWLEDGEMENTS

MA, BB, and AŠ acknowledge funding by the Volkswagen Foundation Grant Az 96727. FF acknowledges financial support by the NOMIS foundation. AŠ acknowledges funding by ERC Starting Grant “NEPA” 802960. We thank Claudia Flandoli for help with illustrations.

[1] R. Phillips, J. Kondev, J. Theriot, and H. Garcia, *Physical biology of the cell* (Garland Science, New York, 2012).

[2] H. T. McMahon and J. L. Gallop, Membrane curvature and mechanisms of dynamic cell membrane remodelling, Nature **438**, 590 (2005).

[3] S. B. Gould, Membranes and evolution, Curr. Biol. **28**, R381 (2018).

[4] S.-V. Albers and B. H. Meyer, The archaeal cell envelope, Nat. Rev. Microbiol. **9**, 414 (2011).

[5] K. Rastädter, D. J. Wurm, O. Spadiut, and J. Quehenberger, The Cell Membrane of Sulfolobus spp.—Homeoviscous Adaption and Biotechnological Applications, International Journal of Molecular Sciences **21**, 3935 (2020).

[6] P. L.-G. Chong, Archaebacterial bipolar tetraether lipids: Physico-chemical and membrane properties, Chem. Phys. Lipids **163**, 253 (2010).

[7] Y. H. Kim, G. Leriche, K. Diraviyam, T. Koyanagi, K. Gao, D. Onofrei, J. Patterson, A. Guha, N. Gianneschi, G. P. Holland, M. K. Gilson, M. Mayer, D. Sept, and J. Yang, Entropic effects enable life at extreme temperatures, Sci. Adv. **5**, eaaw4783 (2019).

[8] P. M. Oger and A. Cario, Adaptation of the membrane in Archaea, Biophys. Chem. **183**, 42 (2013).

[9] M. F. Siliakus, J. van der Oost, and S. W. M. Kengen, Adaptations of archaeal and bacterial membranes to variations in temperature, pH and pressure, Extremophiles **21**, 651 (2017).

[10] D. W. Grogan, Phenotypic characterization of the archaebacterial genus sulfolobus: comparison of five wild-type strains, J. Bacteriol. **171**, 6710 (1989).

[11] T. Hatano, S. Palani, D. Papatziamou, R. Salzer, D. P. Souza, D. Tamarit, M. Makwana, A. Potter, A. Haig, W. Xu, D. Townsend, D. Rochester, D. Bellini, H. M. A. Hussain, T. J. G. Ettema, J. Löwe, B. Baum, N. P. Robinson, and M. Balasubramanian, Asgard archaea shed light on the evolutionary origins of the eukaryotic ubiquitin-ESCRT machinery, Nat. Commun. **13**, 3398 (2022).

[12] D. A. Baum and B. Baum, An inside-out origin for the eukaryotic cell, BMC Biol. **12**, 76 (2014).

[13] M. van Wolferen, A. A. Pulschen, B. Baum, S. Gribaldo, and S.-V. Albers, The cell biology of archaea, Nat. Microbiol. 10.1038/s41564-022-01215-8 (2022).

[14] U. Bakowsky, U. Rothe, E. Antonopoulos, T. Martini, L. Henkel, and H.-J. Freisleben, Monomolecular organization of the main tetraether lipid from Thermoplasma acidophilum at the water–air interface, Chem. Phys. Lipids **105**, 31 (2000).

[15] D. P. Brownholland, G. S. Longo, A. V. Struts, M. J. Justice, I. Szleifer, H. I. Petrache, M. F. Brown, and D. H. Thompson, Phase Separation in Binary Mixtures of Bipolar and Monopolar Lipid Dispersions Revealed by 2H NMR Spectroscopy, Small Angle X-Ray Scattering, and Molecular Theory, Biophysical Journal **97**, 2700 (2009).

[16] C. Jeworrek, F. Evers, M. Erlkamp, S. Grobelny, M. Tolan, P. L.-G. Chong, and R. Winter, Structure and Phase Behavior of Archaeal Lipid Monolayers, Langmuir **27**, 13113 (2011).

[17] V. Vitkova, D. Mitkova, V. Yordanova, P. Pohl, U. Bakowsky, G. Staneva, and O. Batishchev, Elasticity and phase behaviour of biomimetic membrane systems containing tetraether archaeal lipids, Colloids Surf. A Physicochem. Eng. Asp. **601**, 124974 (2020).

[18] E. Chang, Unusual thermal stability of liposomes made from bipolar tetraether lipids, Biochem. Biophys. Res. Commun. **202**, 673 (1994).

[19] O. V. Batishchev, A. S. Alekseeva, D. S. Tretiakova, T. R. Galimzyanov, A. Y. Chernyadyev, N. R. Onishchenko, P. E. Volynsky, and I. A. Boldyrev, Cyclopentane rings in hydrophobic chains of a phospholipid enhance the bilayer stability to electric breakdown, Soft Matter **16**, 3216 (2020).

[20] U. Seifert, Configurations of fluid membranes and vesicles, Adv. Phys. **46**, 13 (1997).

[21] H. Noguchi, Membrane Simulation Models from Nanometer to Micrometer Scale, J. Phys. Soc. Jpn. **78**, 041007 (2009).

[22] F. Frey and T. Idema, More than just a barrier: using physical models to couple membrane shape to cell function, Soft Matter **17**, 3533 (2021).

[23] M. Bulacu, X. Périole, and S. J. Marrink, In Silico Design of Robust Bolalipid Membranes, Biomacromolecules **13**, 196 (2012).

[24] C. Huguet, S. Fietz, A. Rosell-Melé, X. Daura, and L. Costenaro, Molecular dynamics simulation study of the effect of glycerol dialkyl

glycerol tetraether hydroxylation on membrane thermostability, Biochimica et Biophysica Acta (BBA) - Biomembranes **1859**, 966 (2017).

[25] T. R. Galimzyanov, P. I. Kuzmin, P. Pohl, and S. A. Akimov, Elastic deformations of bolalipid membranes, Soft Matter **12**, 2357 (2016).

[26] I. R. Cooke and M. Deserno, Solvent-free model for self-assembling fluid bilayer membranes: Stabilization of the fluid phase based on broad attractive tail potentials, J. Chem. Phys. **123**, 224710 (2005).

[27] P. L.-G. Chong, U. Ayesa, V. Prakash Daswani, and E. C. Hur, On Physical Properties of Tetraether Lipid Membranes: Effects of Cyclopentane Rings, Archaea **2012**, 1 (2012).

[28] A. P. Thompson, H. M. Aktulga, R. Berger, D. S. Bolintineanu, W. M. Brown, P. S. Crozier, P. J. in 't Veld, A. Kohlmeyer, S. G. Moore, T. D. Nguyen, R. Shan, M. J. Stevens, J. Tranchida, C. Trott, and S. J. Plimpton, LAMMPS - a flexible simulation tool for particle-based materials modeling at the atomic, meso, and continuum scales, Comput. Phys. Commun. **271**, 108171 (2022).

[29] A. Stukowski, Visualization and analysis of atomistic simulation data with ovito–the open visualization tool, Modelling and Simulation in Materials Science and Engineering **18**, 015012 (2009).

[30] E. R. May, A. Narang, and D. I. Kopelevich, Role of molecular tilt in thermal fluctuations of lipid membranes, Physical Review E **76**, 021913 (2007).

[31] W. Helfrich, Elastic Properties of Lipid Bilayers: Theory and Possible Experiments, Z. Naturforsch. C **28**, 693 (1973).

[32] M. Hamm and M. Kozlov, Elastic energy of tilt and bending of fluid membranes, Eur. Phys. J. E **3**, 323 (2000).

[33] M. Deserno, Fluid lipid membranes: From differential geometry to curvature stresses, Chemistry and Physics of Lipids **185**, 11 (2015).

[34] V. A. Harmandaris and M. Deserno, A novel method for measuring the bending rigidity of model lipid membranes by simulating tethers, The Journal of Chemical Physics **125**, 204905 (2006).

[35] M. Hu, J. J. Briguglio, and M. Deserno, Determining the Gaussian Curvature Modulus of Lipid Membranes in Simulations, Biophys. J. **102**, 1403 (2012).

[36] M. Tourte, P. Schaeffer, V. Grossi, and P. M. Oger, Functionalized Membrane Domains: An Ancestral Feature of Archaea?, Front. Microbiol. **11**, 526 (2020).

[37] M. Deserno, Elastic deformation of a fluid membrane upon colloid binding, Phys. Rev. E **69**, 031903 (2004), arXiv: cond-mat/0303656.

[38] T. B. H. Schroeder, G. Leriche, T. Koyanagi, M. A. Johnson, K. N. Haengel, O. M. Eggenberger, C. L. Wang, Y. H. Kim, K. Diraviyam, D. Sept, J. Yang, and M. Mayer, Effects of lipid tethering in extremophile-inspired membranes on H(+)/OH(-) flux at room temperature, Biophys. J. **110**, 2430 (2016).

[39] R. Xu, A. Dehghan, A.-C. Shi, and J. Zhou, Elastic property of membranes self-assembled from diblock and triblock copolymers, Chem. Phys. Lipids **221**, 83 (2019).

[40] Z. Dogic and S. Fraden, Ordered phases of filamentous viruses, Curr. Opin. Colloid Interface Sci. **11**, 47 (2006).

[41] E. Barry and Z. Dogic, Entropy driven self-assembly of nonamphiphilic colloidal membranes, Proc. Natl. Acad. Sci. U.S.A. **107**, 10348 (2010).

[42] A. J. Balchunas, R. A. Cabanas, M. J. Zakhary, T. Gibaud, S. Fraden, P. Sharma, M. F. Hagan, and Z. Dogic, Equation of state of colloidal membranes, Soft Matter **15**, 6791 (2019).

[43] M. Amaral, archaeal_membranes : code and examples (2024), available at `https://github.com/Saric-Group/archaeal_membranes`.

[44] M. F. Ergüder and M. Deserno, Identifying systematic errors in a power spectral analysis of simulated lipid membranes, The Journal of Chemical Physics **154**, 214103 (2021).